Incorporation of Fe(III)-IIPs (Ion Imprinted Polymers) and PVA/Gelatine Nanofiber using Electrospinning Method: A Report

Ihsan Alfikro[1], Nopa Afrizal[2], Jorena[3], Khairul Saleh[4], Octavianus Cakra Satya[5], Frinsyah Virgo[6], Idha Royani[7]

{trafalgarihsan@gmail.com[1], nopaafrizal66@gmail.com[2], jorena@mipa.unsri.ac.id[3], khairul_saleh@unsri.ac.id[4], octavianus.satya@mipa.unsri.ac.id[5], frinsyahvirgo@mipa.unsri.ac.id[6], idharoyani@unsri.ac.id}

Department of Physics, Faculty of Mathematics and Natural Sciences, Sriwijaya University, Indralaya Ogan Ilir, Palembang, South Sumatra 30662, Indonesia[1,2,3,4,5,6,7]
Laboratory of Material Science, Department of Physics, Faculty of Mathematics and Natural Sciences, Sriwijaya University, South Sumatera, Indonesia[1,2,3,7]

Corresponding author: idharoyani@unsri.ac.id

Abstract. The incorporation of imprinted polymers and electrospun nanofiber, which aims for continuous and better water treatment, has been quite challenging these days. But with a simple incorporating method, it can be achieved. This study was conducted to incorporate these technologies, with simple suspended method of Fe(III)-IIPs within PVA/GE pre-electrospinning solution. The process was carried out within 15kV, 0.25 mL/h, 55% RH, and 12 cm distance in electrospinning settings. The FTIR characterization showed quite identical spectra, indicating a stabilized polymeric network. SEM imaging showed linked fibers through spherical Gelatine encapsulation, with most pore size distributions below 100 nm. EDS analysis clearly detects the trace of iron element within the nanofiber mats, from the suspended particle of Fe(III)-IIPs, hence it can be stated that the incorporation method has succeeded in bringing Fe(III)-IIPs into nanofiber mats. The study also pointed constructive suggestion in accordance of poorly substrate selection for better characterization data.

Keywords: Imprinted Polymers, Electrospun Nanofiber, Fe(III), PVA, Substrate

1. Introduction

Environmental contamination is a serious problem that accompanies the life of our society as residues from various human activities. One of the vital elements prone to pollution is water, especially in big cities with high industrialization. The consequences of these industry activities, one of them, are an increase of heavy metal contaminants, that are highly toxic, nondegradable, and able to bioaccumulate in the human body [1]. Without proper treatment, heavy metal residues discharged directly or indirectly into the environment will accumulate in lakes, rivers, and seas, or even be absorbed into groundwater [2]. Iron is one of the most common heavy

SICBAS 2023, November 03, Palembang, Indonesia

DOI 10.4108/eai.3-11-2023.2347974

metals that pollute water because of its no. 4 abundance in the earth's crust [3]. As mentioned by Ministry of Health of Indonesia Government in *Peraturan Menteri Kesehatan Republik Indonesia Nomor 2 Tahun 2023 tentang Peraturan Pelaksanaan Peraturan Pemerintah Nomor 66 Tahun 2014 Tentang Kesehatan Lingkungan*, the threshold level of Iron in drinking water is 0.2 ppm [4]

In order to overcome such problem, scientists had developed various methods to separate iron pollutant from water, some of them are coagulation, filtration, precipitation, ozonation, ion exchange, reverse osmosis, and advance oxidation. But those methods are followed by several weaknesses, in which limit their utilization, such as requirement of high-energy equipment, expensive process, and inefficiency metal disposal [5]. Between those methods, adsorption can be applied to cover those weaknesses, because it is low-cost, simple, efficient, and eco-friendly [6]. The adsorption method using solid adsorbent to adsorb iron pollutant to its material surface [7].

One of the material with the principle of adsorption-based is Ion Imprinted Polymers (IIPs), which utilize the printed cavities on its surface to selectively bind iron pollutant. Ion Imprinted Polymers (IIPs) have exceptional advantages, which are comprehensive application, [8] good durability and reusability [9], simple synthesis and low cost process [9], also high selectivity of target molecule [10]. However, Ion Imprinted Polymers (IIPs) are still covered by some weaknesses, which are low adsorption capacity, slow mass-transfer rates, and prolonged adsorption process, because of lacking printed cavities on its surface [11,12]. Therefore, it is necessary to apply nanotechnology to IIPs, not only to reduce their particle size but also to change their material structure. One of the nanostructures that is gaining attention is nanofiber.

Nanofiber is a nanomaterial whose structure forms a fiber, which has a fiber diameter ranging from 10 - 1000 nm [13,14]. Recent trends, nanofiber has been applied to many fields, including energy storage [15], wastewater treatment [16], air filtration [17], tissue engineering [18], food packaging [19], and as a catalyst agent [20]. This is owing to their extraordinary characteristics, including high surface area and porous surface structure (Sudirman et al., 2020). Based on these characteristics, the adsorption capacity of IIPs was shown can be enhanced through their incorporation with nanofiber [21,22].

Among the different methods to synthesize nanofiber, electrospinning method is proven to show the most efficient result, simple process, comprehensive application, and easiness of fiber modification, including controllable size, diverse morphologies, and composite forming with other materials [16,23]. The quality of electrospun nanofiber is influenced by various parameters, including internal parameters (voltage, flow rate, needle-to-collector distance, humidity) and external parameters (concentration, conductivity, viscosity, surface tension of the solution) [14].

Various techniques have been conducted to effectively incorporate IIPs and nanofiber technology. Li et al. [24] incorporated Chitosan-GA (glutaraldehyde) nanofiber (NF) with Pb(II)-containing solution and the nanofiber mats showed an increase up to 50% of adsorption capacity compare to non-imprinted mats, but it's need a post-treatment to imprint Pb^{2+} ion

cavities onto surface of the mats. The similar synthesis technique has been conducted by Rajhans et al. [25], using combination of PVDV-RTIL in Eu(III)-containing solution, but it was stated that during the electrospinning process, the Eu^{3+} ions leave the surface of PVDF-RTIL nanofibers, result in imprinted sites of Eu^{3+} ions on the surface of mats. However, Rajhans et al. [25] do not state why would this event had happened in their work. The other incorporation technique has also existed, involving IIPs with predetermined metal ions imprinted sites, then simple homogenization of IIPs in pre-electrospinning polymer solution [12,26].

Here in this work, we present simple incorporation of two technologies, based on incorporation technique present by Rammika et al [12]. Owing to their biodegradable and non-toxicity characteristics [18], we compromised PVA as the main polymer and combine it with Gelatine as additive agent to increase its viscosity, so it's more electrospinnable. Then incorporate it to Fe(III)-IIPs as ferric ion adsorptive agent. Fe(III)-IIPs@PVA/GE-NF as the final result, is being characterized using XRD, SEM, and FTIR.

2. Method

2.1. Chemicals and Instrumentation

Methacrylic acid (MAA), ethylene glycol dimethacrylate (EGDMA), Ferric Nitrate Nonahydrate [$Fe(NO_3)_3 9H_2O$], benzoyl peroxide (BPO), hydrochloric acid (37% HCl), poly(vinyl) alcohol (PVA) with 98% DH (degree of hydrolysis), Gelatine, and gradient grade of Ethanol were obtained from Sigma Aldrich, and have been used directly without further purification. Typical instrumentations have been used to characterized our materials were FTIR Prestige 21 Shimadzu, XRD Rigaku Miniflex 600, and Hitachi FlexSEM 1000, also the electrospinning apparatus Nachriebe 601 (Nachriebe, Center of Aerosol and Analytical Instrumentation, Department of Physics, ITB, Bandung, Indonesia) was used to synthesized nanofiber mats.

2.2. Synthesis of Fe(III)-IIPs

We demonstrated the most-efficient polymerization method to synthesize the polymeric backbone of Fe(III)-IIPs to substitute nitrogen utility to make oxygen-free solution, by simple cooling treatment in refrigerator [27]. Pre-polymerization solution is prepared by mixing 0.4 mL MAA, 3.9 mL EGDMA, and 0.07 g BPO to 40 mL of 1% Fe^{3+} ion solution in ethanol, consecutively. Then the solution was stored in vials and kept refrigerated on -5°C for an hour, as removal of oxygen occurred by cooling process. Furthermore, the polymerization process was conducted consecutively, on 75°C for 3 h, 80°C for 2 h, and 85°C for an hour to solidification of polymer. A similar process was done to synthesize NIPs (Non-Imprinted Polymers) as control polymer, without $Fe(NO_3)_3$ addition [28].

The solidified polymer was grounded to a fine powder with brown in color and then washed using ethanol and deionized water to remove impurity material on it. The imprinted process of Fe^{3+} ions was conducted by repeated leaching process: 7×50 mL of 6 M HCl and stirred at 60°C

for 18 hours until the precipitation becomes white. This color changes indicated that Fe^{3+} ions have been removed from the polymer body [29].

2.3. Electrospinning Process

Gelatine (GE) was dissolved in 10°C distilled water at 250 rpm automatically stirring in magnetic stirrer with 2.5% concentration, until it completely dissolved. 7.5% PVA powder (relative to the weight of 2.5% GE) was added to the homogeneous solution. Then, stirring process was continued at 85°C temperature, for an hour to dissolve the powder of PVA, to form a homogeneous solution of PVA/GE 7.5/2.5 weight%.

Incorporation of IIPs and nanofiber mats, was carried on by simple suspended of 200 mg Fe(III)-IIPs powder to the 20 mL solution of PVA/GE for 15 min stirring at 50°C. The electrospinning process was carried out at room temperature with 60% RH (relative humidity). Then the parameters were set to 0.25 mL/h flow rate, 15 kV voltage, and 12 cm of tip-to-collector distance. A sheet of aluminium foil was used as the mats collector substrate. The formed nanofiber mats, Fe(III)-IIPs@PVA/GE-NF, on the foil were dried out overnight for further characterization.

2.4. Analysis Method

We conducted analysis based on Rietveld refinement on XRD spectra of Fe(III)-IIPs and Fe(III)-IIPs@PVA/GE-NF by applying the raw data of each diffraction pattern to Profex software [30]. Then utilizing built-in statistical parameters of Profex to search for the best match of crystal phase from local Crystallography Open Database (COD). For the distribution of cavities from SEM imaging, ImageJ version 1.54f was being used to retrieve the data within self-selected diameter range of the cavities [31].

3. Results and Discussion

3.1. FTIR Characterization

In the need of knowing the chemical structure of the samples, the facile and rapid method, FTIR, was used. It's utilize infrared wave, which is wave spectrum at a lower energy range, to study the chemical composition of material based on the vibrational motion of functional group of material [32].

The FTIR spectra of NIPs, Fe(III)-IIPs, and Fe(III)-IIPs@PVA/GE-NF are shown in Figure 1. Each sample showed quite identical FTIR spectra, thus an indication of the stability polymeric network during polymerization [29]. There is a broaden absorbance band at 3520-3380 cm^{-1}, followed by peaks at 1600-1300 cm^{-1}, 1200-1000 cm^{-1}, and 800-600 cm^{-1} on each sample, which confirmed stretching vibration of –OH bond from hydroxyl group [32,33], indicated the existence of ethanol solvent of alcoholic family [34]. As well, a strong absorption of Fe(III)-IIPs@PVA/GE-NF at 3388.93 cm^{-1}, clearly indicated the rich content of hydroxyl groups in PVA polymers [35]. Table 1 shows wavenumber related to each functional group and its absorption.

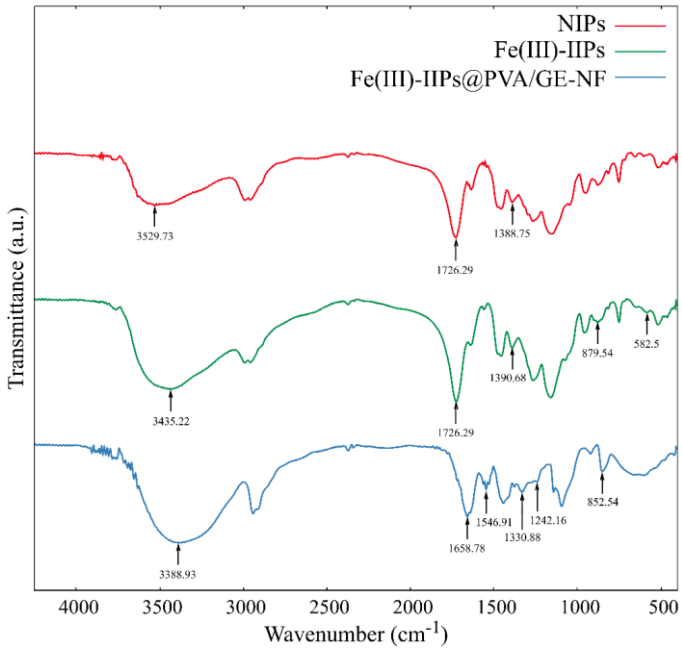

Fig. 1. FTIR Spectra of NIPs, Fe(III)-IIPs, and Fe(III)-IIPs@PVA/GE-NF

The existence of Methacrylic acid (MAA) as a functional monomer confirmed by C=O group at 1726 cm^{-1} from carboxylic acid [36]. And the same functional group has been confirmed in Fe(III)-IIPs@PVA/GE-NF at 1658.78 cm^{-1}, followed by bands at 1546.91 and 1242.16 cm^{-1}, related to stretching C–N amide group and bending of N–H group, which shows the characteristic peaks of Gelatine [18]. Wavenumber of 1380-1350 cm^{-1}, followed by 840-815 cm^{-1} peaks confirmed asymmetric stretching of NO_3^- functional group from common inorganic ion [32,37] in all samples, but those are can also confirm the isopropyl group of alcohol, $–CH(CH_3)_2$ [33].

Table 1. List of functional groups

Functional Group	NIP		Fe(III)-IIPs		Fe(III)-IIPs@PVA/GE-NF	
	k (cm^{-1})	abs (%)	k (cm^{-1})	abs (%)	k (cm^{-1})	abs (%)
–OH (Hydroxyl)	3529.73	36.411	3435.22	62.085	3388.93	67.42
C=O (Carboxylate)	1726.29	58.431	1726.29	70.913	1658.78	49.576
Amide C–N	-	-	1558.48	7.629	1546.91	30.749
N–H bending	1265.3	47.133	1267.23	56.247	1242.16	25.672
NO_3^-/$–CH(CH_3)_2$	1388.75	65.77	1390.68	65.896	1330.88	32.634
Fe-O (Iron oxide)	-	-	582.5	9.869	-	-

The iron content in the polymer structure cannot explicitly be determined by FTIR spectra analysis, commonly for all metallic elements; however the presence of Fe^{3+} can be traced along their interaction with other groups. Beside the confirmation of MAA at 1726 cm^{-1} peak, stronger peak of carboxylic acid within Fe(III)-IIPs sample compare to NIP, indicates the increase of

carboxylic acid content. As proposed by Stodt et al. [35], this increase might be due to the oxidation of alcohol, because the high presence of Fe^{3+} acts as a catalyst in Fe(III)-IIPs, leading to the formation of carboxylic acids.

Wavenumber at 582.5 cm^{-1} in Fe(III)-IIPs resembles to the main spectra of iron-primary-source mineral, i.e. Magnetite [38,39]. Yet it has occurred as iron oxide (Fe-O) and in low absorption, which indicates the interaction of a slight amount of Fe^{3+} with oxygen [40], as a consequence of repeated leaching process beforehand. Due to the absence or lack of sufficient used iron during synthesizing process, NIP and Fe(III)-IIPs@PVA/GE-NF clearly do not show the Fe^{3+} absorption spectra.

3.2. XRD Characterization

XRD spectra of Fe(III)-IIPs and Fe(III)-IIPs@PVA/GE-NF are shown in Figure 2. High intensity peak showed strong constructive interference of X-rays on the sample. This kind of interference is due to X-rays scattering by electrons in the material, which initiated superposition between those waves, so that a higher intensity of that angle recorded than others [41,42]—later called diffraction intensity. Higher recorded intensities of XRD graph, resulted on higher electron density of the material [43].

The XRD spectra of Fe(III)-IIPs and Fe(III)-IIPs@PVA/GE-NF are shown in Figure 2. Peak of Fe^{3+} ions have been confirmed at 14.18° with (020) hkl indices from Lepidocrocite mineral phase in Fe(III)-IIPs sample [30], with the maximum recorded intensity is at 113 cps. This is far smaller than the same material in [44], with the maximum intensity of approx. 950 cps. It was pointed the less content of Fe^{3+} ions in our work related to the conducted leaching treatment.

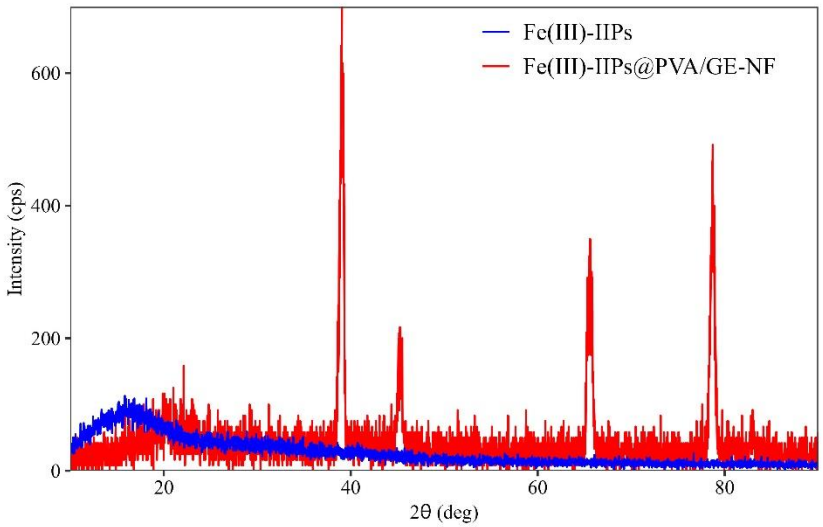

Fig. 2. XRD Spectra of Fe(III)-IIPs@PVA/GE-NF

However, there is a noteworthy difference of both spectra, as a result of characterized materials. High intensity of diffraction with narrow and sharp peaks are recorded in Fe(III)-

IIPs@PVA/GE-NF sample, therefore it can be inferred that the high crystallinity content is presented as a material intrinsic feature. The recorded peaks are responsible for the aluminium content in the material, which is originated from the substrate used along the process. The EDS results have also confirmed this, as state in Figure 3.

3.3. SEM Characterization

Fe(III)-IIPs is characterized by SEM to generate two-dimensional (2D) image of the specific material surface. From this generated image, we can perform analysis to find out the size of cavities which being imprinted on the surface. The image can be segmented into two parts, according to brightness levels. These level are identified from the different contrast color of solids and cavities.

The morphology of Fe(III)-IIPs and Fe(III)-IIPs@PVA/GE-NF are shown in the Figure 3(a) and (b). The leaching process formed the surface of the material into chunks accompanied by clearly seen cavities, as shown on the morphology of Fe(III)-IIPs. Those cavities are formed to recognize Fe^{3+} ions in the environment and bound it to the material surface, which decreased the trace amount of iron pollutant, as consequences of binding process [29]. The more cavities on the surface, result in higher performance of Fe(III)-IIPs to binding iron pollutant to its surface.

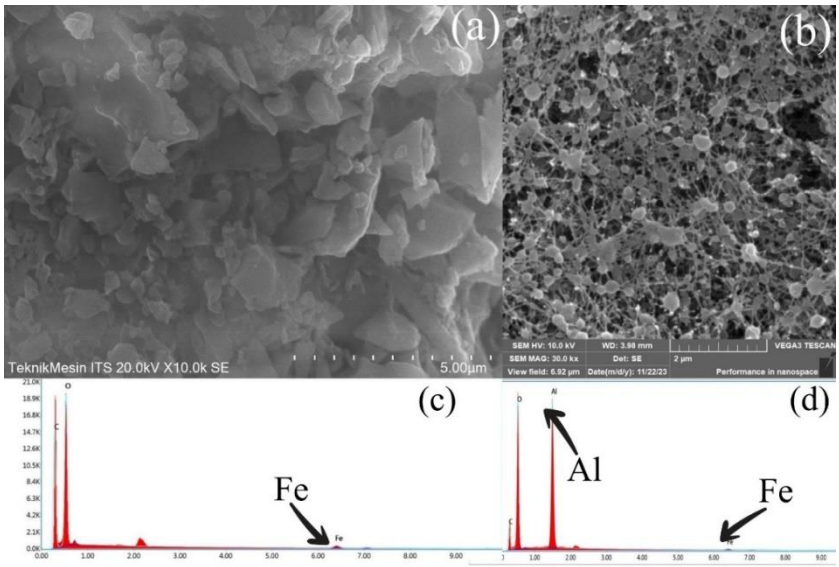

Fig. 3. SEM Imaging of (a) Fe(III)-IIPs and (b) Fe(III)-IIPs@PVA/GE-NF, also EDS Spectra of (c) Fe(III)-IIPs and (d) Fe(III)-IIPs@PVA/GE-NF

SEM imaging also confirms the formation of vaguely interconnected fibers with approx. 38 nm in diameter, linked the configuration of a spherical-like shape, as we called beads, which dominate the surface of Fe(III)-IIPs@PVA/GE-NF. These beads are formed as consequences of the addition of Gelatine in the PVA polymeric network, thus result in agglomeration of Gelatine

protein encapsulated by elongated PVA fibers subjected to electrostatic force, linked each bead [18]. Furthermore, these encapsulated Gelatine might inhibit the formation of thicker fibers.

The EDS spectra of both materials are shown in the Figure 3(c) and (d). It was clearly displayed that atomic bonding of Fe(III)-IIPs are dominated by carbon and oxygen, with the minor intensity of iron, remains within the polymer in the trace amount. The same things are also present in the Fe(III)-IIPs@PVA/GE-NF sample, hence it can be stated that the incorporation method has succeeded bringing Fe(III)-IIPs into PVA/GE electrospun nanofibers, highlighting the content of Fe^{3+} remnant which contained in Fe(III)-IIPs@PVA/GE-NF sample. For a better understanding of the exact fractional quantity of each element within both samples, are shown in Table 2.

Table 2. Quantity fraction of each element

Element	Weight%	
	Fe(III)-IIPs	IIPs@PVA/GE-NF
C K	37.42	19.22
O K	58.39	49.28
FeK	4.19	1.46
AlK	0	30.05
Total %	100	100

A quite dominant of aluminium elements within Fe(III)-IIPs@PVA/GE-NF sample, which is mentioned before, this aluminium content corresponds to the substrate used. So we were unable to peel off the fibers from the substrate, probably due to the lack of sufficient thickness of collected fibers on the substrate. However, we suggest either wrapping the foil with plastic wrap or utilizing ungrease baking paper as substrate for ease of fiber detachment, instead of aluminium foil directly.

Figure 4 shows the distribution of cavity size within Fe(III)-IIPs and Fe(III)-IIPs@PVA/GE-NF samples, with the mean sizes are at 61.6 nm and 93.7 nm, consecutively. The computational analysis successfully generated 457 cavities within Fe(III)-IIPs and 831 for Fe(III)-IIPs@PVA/GE-NF in total. More cavities are formed in the surface of fibers, with dominant distribution in the nanoscale (below 100 nm).

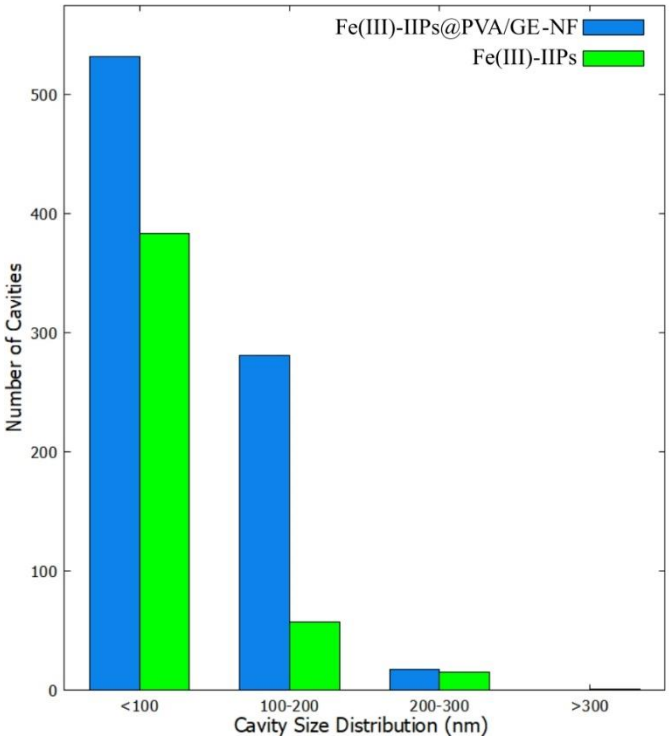

Fig. 4. Cavity Size Distribution of Materials

4. Conclusion

The incorporation of Fe(III)-IIPs within PVA/GE electrospun nanofiber, using a simple method, showed a decent result of incorporated material, as shown by the characterization results. But, we still suffer from data biasness, due to poor substrate selection of pre-electrospinning process. However, the suggestion of the exact substrate selection for better result can dramatically improve the quality of the fibers for further studies.

Acknowledgement

The research/publication of this article was funded by the 2023 Sriwijaya University Public Service Agency DIPA as an additional output. Number SP DIPA-023.17.2.67751512023, On November 30, 2022. In accordance with the Rector's Decree Number: 0188/UN9.3.1/SK/2023, On April 18, 2023".

References

[1] Chheang, L., Thongkon, N., Sriwiriyarat, T., & Thanasupsin S.P.: Heavy Metal Contamination and Human Health Implications in the Chan Thnal Reservoir, Cambodia. Sustainability, Vol. 13, No. 24, pp. 1–20. (2021)

[2] Zhu, F., Zheng, Y.M., Zhang, B.G., & Dai, Y.R.: A critical review on the electrospun nanofibrous membranes for the adsorption of heavy metals in water treatment. Journal of Hazardous Materials, Vol. 401, No. 1, pp. 1–22. (2021)

[3] Khatri, N., Tyagi, S., & Rawtani, D.: Recent strategies for the removal of iron from water: A review. Journal of Water Process Engineering, Vol. 19, No. 5, pp. 291–304. (2017)

[4] Permenkes No. 2 RI.: Peraturan Menteri Kesehatan Republik Indonesia Nomor 2 Tahun 2023 tentang Peraturan Pelaksanaan Peraturan Pemerintah Nomor 66 Tahun 2014 tentang Kesehatan Lingkungan. (2023).

[5] Desta MB.: Batch Sorption Experiments: Langmuir and Freundlich Isotherm Studies for the Adsorption of Textile Metal Ions onto Teff Straw (*Eragrostis tef*) Agricultural Waste. Journal of Thermodynamics, Vol. 2013, No. 3, pp. 1–6. (2013)

[6] Wang, J., & Guo, X.: Adsorption isotherm models: Classification, physical meaning, application and solving method. Chemosphere, Vol. 258, No. 1, pp. 1–25. (2020)

[7] Nageeb, M.: Adsorption Technique for the Removal of Organic Pollutants from Water and Wastewater. In: Rashed MN, editor. Organic Pollutants - Monitoring, Risk and Treatment. 1st ed. (2013).

[8] Kusumkar, V.V., Galamboš, M., Viglašová, E., Daňo, M., & Šmelková, J.: Ion-Imprinted Polymers: Synthesis, Characterization, and Adsorption of Radionuclides. Materials, Vol. 14, No. 5, pp. 1–29. (2021)

[9] Branger, C., Meouche, W., & Margaillan, A.: Recent advances on ion-imprinted polymers. Reactive and Functional Polymers, Vol. 73, No. 6, pp. 859–75. (2013)

[10] Djunaidi, M.C., Haris, A., Pardoyo., & Rosdiana, K.: The Impact of Template Types on Polyeugenol to the Adsorption Selectivity of Ionic Imprinted Polymer (IIP) Fe Metal Ion. In: IOP Conference Series: Materials Science and Engineering. pp. 1–9. (2018)

[11] Patel, K.D., Kim, H.W., Knowles, J.C., & Poma, A.: Molecularly Imprinted Polymers and Electrospinning: Manufacturing Convergence for Next-Level Applications. Advanced Functional Materials, Vol. 30, No. 32, pp. 1–16. (2020)

[12] Rammika, M., Darko, G., & Torto, N.: Incorporation of Ni(II)-Dimethylglyoxime Ion-Imprinted Polymer into Electrospun Polysulphone Nanofibre for the Determination of Ni(II) Ions from aqueous Samples. WSA, Vol. 37, No. 4, pp. 539–46. (2011)

[13] Aghasiloo, P., Yousefzadeh, M., Latifi, M., & Jose, R.: Highly porous TiO_2 nanofibers by humid-electrospinning with enhanced photocatalytic properties. Journal of Alloys and Compounds, Vol. 790, No. 2, pp. 257–65. (2019)

[14] Matsuura, T., Shirazi, M.M.A.: Principles of Electrospinning and Nanofiber Membranes. In: Kargari A, editor. Electrospun and Nanofibrous Membranes, 1st ed. pp. 3–25. (2023).
[15] Almafie, M.R., Marlina, L., Riyanto, R., Jauhari, J., Nawawi, Z., & Sriyanti I.: Dielectric Properties and Flexibility of Polyacrylonitrile/Graphene Oxide Composite Nanofibers. ACS Omega, Vol. 7, No. 37, pp. 33087–96. (2022)
[16] Ardekani, R., Borhani, S., & Rezaei, B.: Selective molecularly imprinted polymer nanofiber sorbent for the extraction of Bisphenol A in a water sample. Polymer International, Vol. 69, No. 9, pp. 780–93. (2020)
[17] Zulfi, A., Hapidin, D.A., Munir, M.M., Iskandar, F., & Khairurrijal, K.: The synthesis of nanofiber membranes from acrylonitrile butadiene styrene (ABS) waste using electrospinning for use as air filtration media. RSC Advances, Vol. 9, No. 53, pp. 30741–51. (2019)
[18] Perez-Puyana, V., Jiménez-Rosado, M., Romero, A., & Guerrero, A.: Development of PVA/gelatin nanofibrous scaffolds for Tissue Engineering via electrospinning. Materials Research Express, Vol. 5, No. 3, pp. 1–8. (2018)
[19] Pandey, V.K., Upadhyay, S.N., Niranjan, K., Mishra, P.K.: Antimicrobial biodegradable chitosan-based composite Nano-layers for food packaging. International Journal of Biological Macromolecules, Vol. 157, pp. 212–219. (2020)
[20] Nasikhudin., Diantoro, M., Kusumaatmaja, A., & Triyana, K.: Study on Photocatalytic Properties of TiO_2 Nanoparticle in various pH condition. In: Journal of Physics: Conference Series. pp. 1–7. (2018)
[21] Zaidi, S.A.: Recent Developments in Molecularly Imprinted Polymer Nanofibers and Their Applications. Analytical Methods, Vol. 7, No. 18, pp. 7406–7415. (2015)
[22] Gore, P.M., Khurana, L., Siddique, S., Panicker, A., & Kandasubramanian, B.: Ion-imprinted electrospun nanofibers of chitosan/1-butyl-3-methylimidazolium tetrafluoroborate for the dynamic expulsion of thorium (IV) ions from mimicked effluents. Environmental Science and Pollution Research, Vol. 25, No. 4, pp. 3320–3334. (2018)
[23] Rajak, A., Hapidin, D.A., Iskandar, F., Munir, M.M., & Khairurrijal, K.: Electrospun nanofiber from various source of expanded polystyrene (EPS) waste and their characterization as potential air filter media. Waste Management, Vol. 103, No. 1, pp. 76–86. (2020)
[24] Li, Y., Zhang, J., Xu, C., & Zhou, Y.: Crosslinked chitosan nanofiber mats fabricated by one-step electrospinning and ion-imprinting methods for metal ions adsorption. Science China Chemistry, Vol. 59, No. 1, pp. 95–105. (2016)
[25] Rajhans, A., Gore, P.M., Siddique, S.K., & Kandasubramanian, B.: Ion-imprinted nanofibers of PVDF/1-butyl-3-methylimidazolium tetrafluoroborate for dynamic recovery of Europium(III) ions from mimicked effluent. Journal of Environmental Chemical Engineering, Vol. 7, No. 3, pp. 1–12. (2019)
[26] Ding, T., Wu, Q., Nie, Z., Zheng, M., Wang, Y., & Yang, D.: Selective recovery of lithium resources in salt lakes by polyacrylonitrile/ion-imprinted polymer: Synthesis, testing, and computation. Polymer Testing, Vol. 113, No. 1, pp. 1–8. (2022)
[27] Royani, I., Widayani., Abdullah, M., & Khairurrijal.: Characterization of an atrazine molecularly imprinted polymer prepared by a cooling method. In: International Conference on Mathematics and Natural Sciences. pp. 116–9. (2014)
[28] Maimuna, M., Monado, F., & Royani, I.: Studi awal pengaruh kloroform sebagai pelarut pada proses ekstraksi molecularly imprinted polymer (MIP) nano kafein. Jurnal Fisika, Vol. 10, No. 1, pp. 1–7. (2020)
[29] Roushani, M., Beygi, T.M., & Saedi, Z.: Synthesis and application of ion-imprinted polymer for extraction and pre-concentration of iron ions in environmental water and food samples. Spectrochimica Acta Part A: Molecular and Biomolecular Spectroscopy, Vol. 153, No. 1, pp. 637–44. (2016)
[30] Doebelin, N., & Kleeberg, R.: Profex: a graphical user interface for the Rietveld refinement program *BGMN*. Journal of Applied Crystallography, Vol. 48, No. 5, pp. 1573–80. (2015)
[31] Schindelin, J., Arganda-Carreras, I., Frise, E., Kaynig, V., Longair, M., Pietzsch, T., Preibisch, S., Rueden, C., Saalfeld, S., Schmid, B., Tinevez, J., White, D.J., Hartenstein, V., Eliceiri, K.,

Tomancak, P., Cardona, A.: Fiji: an open-source platform for biological-image analysis. Nature Methods, Vol. 9, No. 7, pp. 676–682. (2012)
[32] Nandiyanto, A.B.D., Oktiani, R., & Ragadhita, R.: How to Read and Interpret FTIR Spectroscope of Organic Material. Indonesian Journal Science Technology, Vol. 4, No. 1, pp. 97–118. (2019)
[33] Lingegowda, D.C., Kumar, J.K., Prasad, A.G.D., Zarei, M., & Gopal, S.: FTIR Spectroscopic Studies on Cleome gynandra – Comparative Analysis of Functional Group Before and After Extraction. Romanian Journal of Biophysics, Vol. 22, No. 3, pp. 137–143. (2013)
[34] Brown, T.L., LeMay, Jr. H.E., Bursten, B.E., Murphy, C.J., & Woodward, P.M.: Chemistry: The Central Science. 12th ed. 1050 pages (2012).
[35] Wang, J., Ye, L.: Structure and properties of polyvinyl alcohol/polyurethane blends. Composites Part B: Engineering, Vol. 69, No. 1, pp. 389–96. (2015)
[36] Bow, Y., Sutriyono, E., Nasir, S., & Iskandar, I.: Preparation of molecularly imprinted polymers simazine as material potentiometric sensor. In: Iskandar I., Ismadji S., Agustina TE., Yani I., Komariah LN., Hasyim S, editors. MATEC Web of Conferences. pages 1–5 (2017).
[37] Goebbert, D.J., Garand, E., Wende, T., Bergmann, R., Meijer, G., Asmis, K.R., Neumark, D.M.: Infrared Spectroscopy of the Microhydrated Nitrate Ions $NO_3^-(H_2O)_{1-6}$. The journal of physical chemistry A, Vol. 113, No. 26, pp. 7584–7592. (2009)
[38] Veneranda, M., Aramendia, J., Bellot-Gurlet, L., Colomban, P., Castro, K., & Madariaga, J.M.: FTIR spectroscopic semi-quantification of iron phases: A new method to evaluate the protection ability index (PAI) of archaeological artefacts corrosion systems. Corrosion Science, Vol. 133, pp. 68-77. (2018).
[39] Chirita, M., Banica, R., Ieta, A., & Grozescu, I.: Superparamagnetic Unusual Behavior of Micrometric Magnetite Monodisperse Monocrystals Synthesized by Fe-EDTA Thermal Decomposition. Particulate Science and Technology, Vol. 30, No. 4, pp. 354–363. (2012)
[40] Ahangaran, F., Hassanzadeh, A., & Nouri, S.: Surface modification of $Fe_3O_4@SiO_2$ microsphere by silane coupling agent. International Nano Letters, Vol. 3, No. 1, pp. 1–5. (2013).
[41] Blake, A.J., Cole, J.M., Evans, J.S.O., Main, P., Parsons, S., & Watkin, D.J.: Crystal Structure Analysis: Principles and Practice. 2nd ed. Clegg W, editor. 387 pages (2009).
[42] Waseda, Y., Matsubara, E., Shinoda, K.: X-Ray Diffraction Crystallography: Introduction, Examples, and Solved Problems [Internet]. 1st ed. 310 pages (2011).
[43] Widjonarko, N.: Introduction to Advanced X-ray Diffraction Techniques for Polymeric Thin Films. Coatings, Vol. 6, No. 4, pp. 1–17. (2016)
[44] Kartika, H.D., Jorena, J., Monado, F., & Royani, I.: Analisis Jumlah Rongga Tercetak pada Ion Imprinted Polymer (IIPs)-Fe(III) Yang disintesis menggunakan Metode Cooling-heating. Jurnal Penelitian Sains, Vol. 24, No. 1, pp. 18–23. (2022)